Int J Clin Exp Med 2020;13(3):1389-1397
www.ijcem.com /ISSN:1940-5901/IJCEM0104898

Original Article

TRAF6 and IL-6 disturb the balance between bone formation and bone resorption in ovariectomized osteoporotic mice

Quzhe Lu[1], Meixiuli Li[1], Daiqin Chen[2]

[1]Department of Anatomy Teaching and Research, Shaoyang University, Shaoyang, Hunan, China; [2]Department of Cardiology, Shaoyang Central Hospital, Shaoyang School of Meizilin Campus, Shaoyang, Hunan, China

Received November 14, 2019; Accepted December 26, 2019; Epub March 15, 2020; Published March 30, 2020

Abstract: Objective: To study the expression of tumor necrosis factor receptor associated factor 6 (TRAF6) and interleukin-6 (IL-6) in osteoporotic mice and the effects of these proteins on bone mineral density. Methods: Twenty healthy specific-pathogen-free female BALB/C mice were randomly divided into a model group (n=10) and a sham-operation group (n=10). The total bone mineral density changes and peripheral blood *Traf6* mRNA, TRAF6, *Il6* mRNA, IL-6, Ca^{2+}, and P level changes in the mice were determined before modeling and at 1, 3, 6, and 12 weeks after modeling. Results: The total bone density in the model group was lower than those in the sham-operation group at 3, 6, and 12 weeks after modeling (all $P<0.05$). The levels of *Traf6* mRNA, *Il6* mRNA, and IL-6 in the model group were higher than those in the sham-operation group at 1, 3, 6, and 12 weeks after modeling (all $P<0.05$). Blood Ca^{2+} and P levels in the model group were higher than those in the sham-operation group at 6 and 12 weeks after modeling (all $P<0.05$). Total bone mineral density was negatively correlated with *Traf6* mRNA, *Il6* mRNA, and IL-6 levels in the model group. There was a positive correlation between the blood Ca^{2+} level and *Traf6* mRNA, *Il6* mRNA, and IL-6 levels in the model group. There was a positive correlation between the blood P level and *Traf6* mRNA, *Il6* mRNA, and IL-6 levels in the model group. Conclusion: TRAF6 and IL-6 may participate in the development of osteoporosis in ovariectomized osteoporotic mice by inhibiting bone formation, promoting bone resorption, and reducing bone density and thus disturbing the balance between bone formation and bone resorption.

Keywords: TRAF6, IL-6, osteoporotic mice, bone mineral density

Introduction

Osteoporosis is a systemic metabolic bone disease characterized by a significant decrease in bone mass, often resulting in the degeneration of the bone tissue microstructure and causing an increase in bone fragility and fracture risk [1, 2]. In recent years, with the increasing age of the global population, the incidence of osteoporosis has increased substantially. It is estimated that a fracture caused by osteoporosis occurs every 3 seconds worldwide. Thus, osteoporosis has become a public health burden that greatly affects people's quality of life and is an important cause of disability and even death [3, 4].

Menopause is an important contributor to osteoporosis in women. The combination of estrogen and estrogen receptors plays an important role in the metabolism of bone tissue [5, 6]. Many studies have found that postmenopausal women are prone to osteoporosis which can be relieved by estrogen therapy [7, 8]. However, the exact mechanism of osteoporosis development in postmenopausal women is unclear. Tumor necrosis factor receptor-associated factor 6 (TRAF6) can increase osteoclast levels and enhance bone resorption, and thereby plays an important role in osteoporosis and bone loss [9]. Additionally, the expression of interleukin-6 (IL-6) is increased in patients with osteoporosis. Increased IL-6 levels promote osteogenic disorders of bone marrow mesenchymal stem cells in the vertebral body of diabetic osteoporotic mice [10]. However, there have been few reports on the role of TRAF6 and IL-6 in postmenopausal osteoporosis, which still needs to be explored.

Table 1. Primer sequences for qRT-PCR

	Forward primer	Reverse primer
TRAF6	5'-CGTCCAGAGGACCCAAATTATG-3'	5'-CCCAAAGTTGCCAATCTTCC-3'
IL-6	5'-TCAATGAGGAGACTTGCCTG-3'	5'-GATGAGTTGTCATGTCCTGC-3'
GAPDH	5'-CGGAGTCAACGGATTTGGTCGTAT-3'	5'-AGCCTTCTCCATGGTGGTGAAGAC-3'

Table 2. Total bone mineral density of mice (g/cm^3)

	Sham-operation group	Model group	Statistic	*P*-value
W0	0.0712±0.0034	0.0711±0.0033	0.0667	0.948
W1	0.0723±0.0048	0.0714±0.0028	0.512	0.615
W3	0.0984±0.0053*	0.0882±0.0043*	4.726	<0.001
W6	0.1146±0.0058#	0.0797±0.0036#	11.535	<0.001
W12	0.1203±0.0061	0.0736±0.0058&	13.788	<0.001

Note: *: compared with W1 P<0.05; #: compared with W3 P<0.05; &: compared with W6 P<0.05.

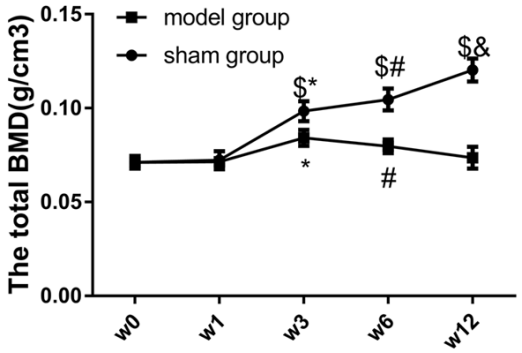

Figure 1. Analysis of total bone mineral density in the two groups of mice. *: comparison at w1, P<0.05; #: comparison at w3, P<0.05; &: comparison at w6, P<0.05. At w3, w6, and w12, the total bone density in the model group was significantly lower than that in the sham-operation group (all P<0.05).

Therefore, the aim of the present study was to study the role of TRAF6 and IL-6 in the pathogenesis of osteoporosis. A mouse model of osteoporosis was established and used to analyze the expression and effects of TRAF6 and IL-6 on bone mineral density. The results of this study will increase our understanding of the clinical mechanism of postmenopausal osteoporosis and provide guidance for more effective treatments.

Materials and methods

Research subjects

Twenty healthy specific-pathogen-free (SPF) female BALB/C mice were purchased from Changzhou Cavens Laboratory Animal Co., Ltd. China, production license number: SCXK (SU) 2011-0003. Mice aged between 65 and 75 days, with a body weight of 18-22 g, were fed irradiated Shuke and Beita SPF grade food (Jiangsu Xietong Pharmaceutical Bioengineering Co., Ltd. China). Drinking water was acidified to a pH value between 2.5-3 after autoclaving. The housing temperature was maintained 26-27°C and the relative humidity at 45-55%. The mice were housed individually in a terrarium, with a change in bedding 1-2 times a week, which included cleaning and disinfection. Noise was maintained below 60 dB, the ammonia concentration in the cage was monitored so that it did not exceed 14 ppm. Ventilation was performed no less than 15 times per hour, and fluorescent lights were used to achieve a 12:12 light-dark cycle. A random number table method was used to divide the mice into a model group and a sham-operation group (both n=10). All animal experiments were approved by the Ethics Committee of Shaoyang Central Hospital.

Establishment of the mouse model

Mice were disinfected on their abdomen and given an intraperitoneal injection of 10% chloral hydrate (300 μg/g body weight) to achieve anesthesia. After anesthesia was satisfactorily accomplished, surgery was performed using a ventral approach. An abdominal incision was made to open the thoracic cavity. For mice in the model group (n=10), the bilateral ovaries were excised. For mice in the sham-operation group (n=10), a small sample of adipose tissue, roughly the same size as the ovaries, was excised. For both groups, the muscles of the lower extremities were injected with lincomycin hydrochloride (0.2 mL, 10 mg/mL) to reduce inflammation. After the mice recovered from anesthesia, they were allowed *ad libitum* access to water and food. Dual-energy X-ray absorptiometry (DXA, formerly DEXA) was used to confirm the establishment of the osteoporo-

Table 3. TRAF6 mRNA levels in mice

	Sham operation group	Model group	Statistic	*P*-value
W0	0.643±0.024	0.639±0.025	0.365	0.719
W1	0.638±0.021	0.712±0.029$^{\Delta}$	2.532	0.030
W3	0.652±0.023	1.003±0.039*	24.515	<0.001
W6	0.644±0.025	1.324±0.041$^{\#}$	44.780	<0.001
W12	0.647±0.022	1.522±0.047$^{\&}$	53.320	<0.001

Note: Δ: compared with W0 P<0.05; *: compared with W1 P<0.05; #: compared with W3 P<0.05; &: compared with W6 P<0.05.

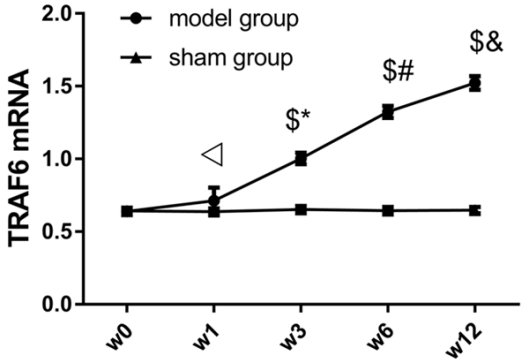

Figure 2. Detection of *Traf6* mRNA in the two groups of mice. r: comparison at w0, P<0.05; *: comparison at w1, P<0.05; #: comparison at w3, P<0.05; &: comparison at w6, P<0.05. The expression level of *Traf6* mRNA in the model group was higher than that in the sham-operation group at all time points (all P<0.05). *Traf6*, tumor necrosis factor receptor associated factor 6.

sis model. If the mean total bone mineral density in the model group was less than twice the standard deviation of the mean total bone mineral density of the sham-operation group (sham-operation group standard deviation), then the model was assessed as being successfully established.

Determining the expression of Traf6 and Il6 mRNA by quantitative real-time reverse transcription polymerase chain reaction (qRT-PCR)

Before modeling (w0), 1 week after modeling (w1), 3 weeks after modeling (w3), 6 weeks after modeling (w6), and 12 weeks after modeling (w12), peripheral blood was sampled from the tail vein of the mice in both groups. RNA was extracted from the peripheral blood using TRIzol reagent (Invitrogen), according to the manufacturer's instructions, using a volume ratio of TRIzol reagent to serum of 3:1. A microultraviolet spectrophotometer DanoProp 1000 (Tommogen Biotech Co., Ltd.) was used to analyze the concentration and purity of the extracted total RNA, and an A260/A280 value between 1.45 and 1.60 was considered to meet the experimental requirements. Agarose gel electrophoresis (1%; Shanghai Lianmai Biological Engineering Co., Ltd.) was performed to assess RNA integrity. The SYBR Green staining method was used to quantitatively analyze mRNA expression levels on the 7300 Sequence Detection System (Applied Biosystems). The reverse transcription reaction was performed using an Omniscript Reverse Transcription Kit (QIAGEN); the reaction conditions were 37°C for 60 minutes and 85°C for 5 minutes. The reaction system comprised 5.0 μL of 5 × Reaction Buffer, 1 μL RTase Mix, 2 μg total RNA, 2 μL of 2.5 U/μL polymerase, and RNA-free distilled water were added to bring the final volume to 25 μL. The first strand cDNA was synthesized and subjected to an amplification reaction. The PCR amplification conditions included initial denaturation at 95°C for 10 minutes; 40 cycles of denaturation at 95°C for 15 seconds, annealing at 60°C, and extension for 1 minute; and a final melting curve analysis cycle at 95°C for 15 seconds, 60°C for 15 seconds, and 95°C for 15 seconds. Brilliant SYBR Green QPCR Master Mix (Applied Biosystems) was used in a 20 μL reaction system comprised of 2 μL of cDNA template, 12 μL of SYBR Green Mix, 2 μL each of upstream and downstream primers, and up to 20 μL of double distilled water. Mouse *Gapdh* (encoding glyceraldehyde-3-phosphate dehydrogenase) was used as the internal reference. Each sample was tested in triplicate, and the results were analyzed using the $2^{-\Delta\Delta Ct}$ method [11]. The primer sequences are shown in **Table 1**.

Detection of IL-6 level using enzyme-linked immunosorbent assay (ELISA)

Mouse peripheral blood was centrifuged to collect the serum. Then, 50 μL of the sample analysis buffer and 50 μL of serum were added to each well of a 96-well plate and incubated for 2 h at room temperature. After incubation, the wells were washed five times, followed by the addition of 100 μL of a biotinylated antibody. The plate was sealed and incubated at room

Table 4. IL-6 mRNA levels in mice

	Sham operation group	Model group	Statistic	*P*-value
W0	0.245±0.019	0.242±0.020	0.344	0.735
W1	0.239±0.020	0.412±0.033$^{\Delta}$	16.570	<0.001
W3	0.241±0.018	0.525±0.036*	22.313	<0.001
W6	0.244±0.021	0.638±0.037$^{\#}$	29.286	<0.001
W12	0.242±0.019	0.762±0.044$^{\&}$	34.310	<0.001

Note: Δ: compared with W0 P<0.05; *: compared with W1 P<0.05; #: compared with W3 P<0.05; &: compared with W6 P<0.05.

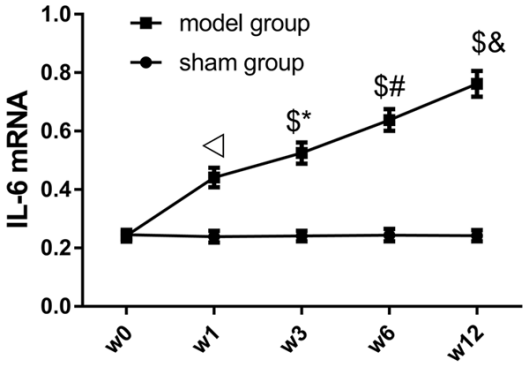

Figure 3. Detection of *Il6* mRNA in the two groups of mice. r: comparison at w0, P<0.05; *: comparison at w1, P<0.05; #: comparison at w3, P<0.05; &: comparison at w6, P<0.05. The expression level of *Il6* mRNA in the model group was higher than that in the sham-operation group at all time points (all P<0.05). *Il6*, interleukin 6.

temperature for 1 h. The wells were then washed, 100 μL of horseradish peroxidase was added to each well, and the plate was incubated for 20 min in the dark. Thereafter, 100 μL of chromogenic substrate 3, 3', 5, 5'-Tetramethylbenzidine (TMB) was added to each well and the plate was incubated at room temperature in the dark for 20 min. Finally, 50 μL of stop buffer was added and the absorbance of each well was read using a microplate reader at 450 nm within 15 min. Three sets of duplicate wells were read, and the experiment was repeated three times. The IL-6 ELISA kit was purchased from BioSource.

Observation indicators

Changes in total bone mineral density and levels of *Traf6* mRNA, TRAF6, *Il6* mRNA, IL-6, Ca^{2+}, and P in the peripheral blood of mice were determined at w0, w1, w3, w6, and w12. The correlations of *Traf6* mRNA, *Il6* mRNA, and IL-6 with total bone mineral density and Ca^{2+} and P levels in the mouse model group at 12 weeks after modeling were assessed. Ca^{2+} and P levels were measured using a Beckman Olympus 5800 automatic biochemical analyzer.

Statistical analysis

SPSS 19.0 (Asia Analytics, formerly SPSS, China) was used to perform the statistical analyses. The numerical data were expressed as the rate, and rates were compared using the χ^2 test. The measured data were expressed as $\bar{x}$ ± SD (standard deviation) and analyzed using Student's t-test. Comparisons within the groups at different time points were analyzed using repeated measures analysis of variance (ANOVA) with post hoc LSD test. Correlations between *Traf6* mRNA, *Il6* mRNA, IL-6, and total bone mineral density and Ca^{2+} and P levels were detected using the Pearson correlation analysis in the model group. P<0.05 indicated a statistically significant difference.

Results

Ovariectomized mice had lower total bone mineral density at w3, w6, and w12

Before modeling (w0), there was no significant difference between the total bone mineral density of the sham-operation and model groups (P > 0.05). After modeling, the total bone mineral density of the sham-operation group showed an upward trend. Comparing two adjacent time points, the total bone density at w3 was higher than that at w1 (P<0.05). The total bone density at w3 was higher than that at w6 (P<0.05). Thereafter, there was no significant difference between the total bone densities at two adjacent time points (P > 0.05). The total bone mineral density also increased in the first three weeks in the model group. The total bone density at w3 was higher than that at w1 (P<0.05). There was no significant difference in bone mineral density between w0 and w1 (P > 0.05). However, after three weeks, the total bone density of the mice in both groups began to decrease. The total bone density at w6 was less than that at w3 (P<0.05), and the total bone density at w12 was less than that at w6 (P<0.05). Comparing the two groups, there was a statistically significant difference in total bone mineral density at w3, w6, and w12, such that the model group had significantly lower bone mineral density than the sham-operation

Table 5. IL-6 levels in mice (pg/ml)

	Sham group	Model group	Statistic	*P*-value
W0	169.42±12.69	168.62±12.57	0.142	0.889
W1	172.44±12.38	245.56±13.47$^{\Delta}$	12.639	<0.001
W3	168.72±12.49	267.43±13.56*	16.932	<0.001
W6	171.33±12.56	301.55±14.02$^{\#}$	21.877	<0.001
W12	167.53±12.62	323.86±14.65$^{\&}$	25.567	<0.001

Note: Δ: compared with W0 P<0.05; *: compared with W1 P<0.05; #: compared with W3 P<0.05; &: compared with W6 P<0.05.

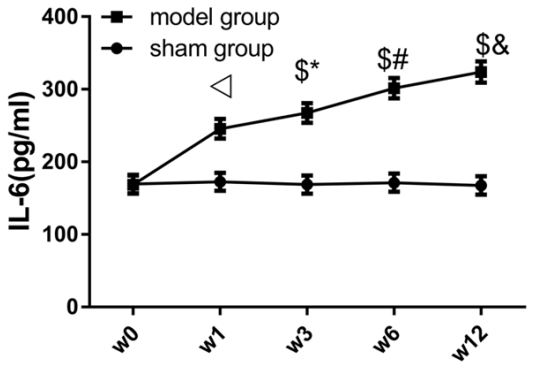

Figure 4. IL-6 protein abundance in the two groups of mice. r: comparison at w0, P<0.05; *: comparison at w1, P<0.05 vs.; #: comparison at w3, P<0.05; comparison at w6, P<0.05. The expression of IL-6 in the model group was significantly higher than that in the sham-operation group at all time points (all P<0.05). IL-6, interleukin 6.

group (all P<0.05). There were no significant differences in total bone mineral density at w1 (P > 0.05) (**Table 2**; **Figure 1**).

Ovariectomized osteoporotic mice had higher Traf6 mRNA expression

There was no significant difference in the relative expression level of *Traf6* mRNA between the model group and the sham-operation group before modeling (w0; P > 0.05). After modelling, the expression level of *Traf6* mRNA in the model group was significantly higher than that in the sham-operation group at all time points (w1, w3, w6, and w12; all P<0.05) (**Table 3**; **Figure 2**).

Ovariectomized osteoporotic mice had higher Il6 mRNA expression

There was no significant difference in the relative expression level of *Il6* mRNA between the two groups of mice before modeling (w0; P > 0.05). After modeling, *Il6* mRNA expression increased gradually in the model group, and there were significant differences between the two groups at all time points (w1, w3, w6, and w12; all P<0.05) (**Table 4**; **Figure 3**).

Ovariectomized osteoporotic mice had higher IL-6 levels

There was no significant difference in the level of IL-6 between the two groups of mice before modeling (w0; P > 0.05). After modeling, the levels of IL-6 in the two groups of mice at w1, w3, w6, and w12 were significantly different, such that the levels of IL-6 in the model group were significantly increased compared to those in the sham-operation group (all P<0.05) (**Table 5**; **Figure 4**).

Ovariectomized osteoporotic mice had higher blood Ca^{2+} levels at w6 and w12

There was no significant difference in blood Ca^{2+} level between the two groups before modeling (w0; P > 0.05). After modeling, the blood Ca^{2+} levels in the model group were significantly lower than those in the sham-operation group at w6 and w12 (P<0.05) (**Table 6**; **Figure 5**). There were no changes at the other time points (w1 and w3).

Ovariectomized osteoporotic mice had higher blood P levels at w6 and w12

There was no significant difference in blood P levels between the two groups of mice before modeling (w0; P > 0.05). After modeling, the levels of blood P in the model group were significantly higher than those in the sham-operation group at w6 and w12 (P<0.05) (**Table 7**; **Figure 6**). There were no changes at the other time points (w1 and w3).

Correlation analysis

Pearson correlation analysis showed that total bone mineral density in the model group was negatively correlated with the levels of *Traf6* mRNA (r=-0.615, P=0.039), *Il6* mRNA (r=-0.740, P=0.015), and IL-6 (r=-0.696, P=0.025). The level of blood Ca^{2+} in the model group was positively correlated with the levels of *Traf6* mRNA (r=0.738, P=0.015), *Il6* mRNA (r=0.811, P=0.004), and IL-6 (P=0.004). The level of

Table 6. Serum Ca^{2+} levels in mice (mmol/L)

	Sham group	Model group	Statistic	*P*-value
W0	2.483±0.204	2.479±0.203	0.044	0.965
W1	2.492±0.203	2.483±0.212	0.312	0.758
W3	2.515±0.206	2.502±0.211	0.397	0.696
W6	2.544±0.211	2.671±0.213#	3.829	0.001
W12	2.585±0.217	2.858±0.209&	6.791	<0.001

Note: #: compared with W3 P<0.05; &: compared with W6 P<0.05. Ca^{2+}: Calcium.

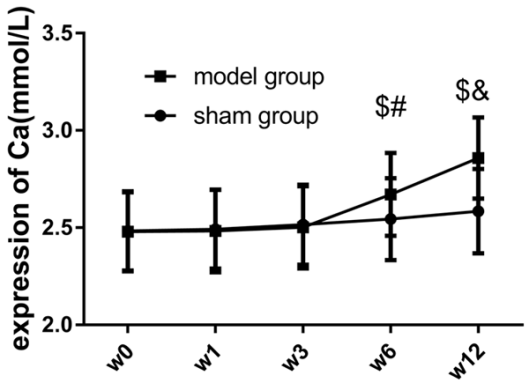

Figure 5. Blood Ca^{2+} levels in the two groups of mice. #: comparison at w3 P<0.05; &: comparison at w6, P<0.05. The blood Ca levels in the model group were significantly higher than those in the sham-operation group at w6 and w12 (P<0.05). Ca, Calcium.

Table 7. Serum P levels in mice (mmol/L)

	Sham group	Model group	Statistic	*P*-value
W0	1.669±0.204	1.672±0.201	0.033	0.974
W1	1.615±0.213	1.689±0.207	0.277	0.785
W3	1.626±0.217	1.718±0.206	1.776	0.093
W6	1.635±0.221	1.932±0.198#	5.361	<0.001
W12	1.653±0.219	2.186±0.194&	8.831	<0.001

Note: #: compared with W3 P<0.05; &: compared with W6 P<0.05. P: Phosphorus.

blood P in the model group was positively correlated with the levels of *Traf6* mRNA (r=0.733, P=0.016), *Il6* mRNA (r=0.851, P=0.002), and IL-6 (r=0.765, P=0.010) in the model group (**Table 8**; **Figure 7**).

Discussion

The risk of osteoporosis increases with increasing age, especially in postmenopausal women. Specifically, menopause, age, and abnormal glucocorticoid secretion are the major risk factors for osteoporosis [12, 13]. Currently, it is

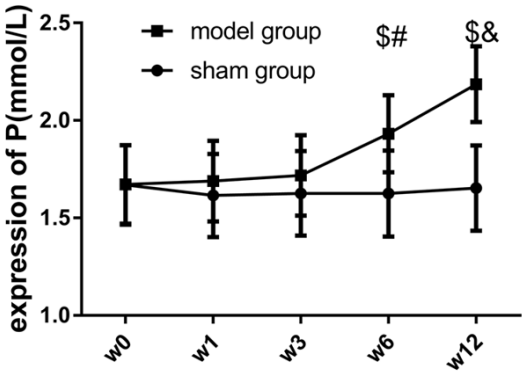

Figure 6. Blood P levels in the two groups of mice. #: comparison at w3 P<0.05; &: comparison at w6, P<0.05. The levels of blood P in the model group were significantly higher than those in the sham-operation group at w6 and w12 (P<0.05). P: Phosphorus.

not possible to completely prevent the occurrence of osteoporosis or cure it. Therefore, studying the mechanism of postmenopausal osteoporosis is important to develop methods to better prevent and treat osteoporosis and avoid serious complications [14, 15]. TRAF6 is closely related to bone metabolism. *Traf6*-deficient mice exhibit osteoclastogenesis defects and severe bone sclerosis [16]. IL-6 is involved in several age-related diseases and plays an important role in the occurrence and development of osteoporosis [17]. The osteoporosis model of ovariectomized female mice used in this study is a classic model of postmenopausal osteoporosis [18]. Therefore, in the present study, we investigated the expression of TRAF6 and IL-6 in osteoporotic mice and examined the effects of these proteins on bone mineral density.

In this study, BALB/C mice were used to establish an ovariectomized osteoporotic model. BALB/C mice generally have no invasive habits, are relatively easy to colonize, and have been bred at global research institutions for more than two hundred generations; thus, they are a credible choice for research [19]. Bone mineral density is the gold standard for the diagnosis of osteoporosis [20]. After modeling, the total bone mineral density of the mice was measured, and the average bone mineral density of the model group was found to be less than twice the standard deviation of the average bone density of the mice in the sham-operation group at 6 weeks after modeling. This indicated

Table 8. Correlation analysis

	Total BMD	Ca^{2+}	P
TRAF6 mRNA	r=-0.615, P=0.039	r=0.738, P=0.015	r=0.733, P=0.016
IL-6 mRNA	r=-0.740, P=0.015	r=0.811, P=0.004	r=0.851, P=0.002
IL-6	r=-0.696, P=0.025	r=0.732, P=0.016	r=0.765, P=0.010

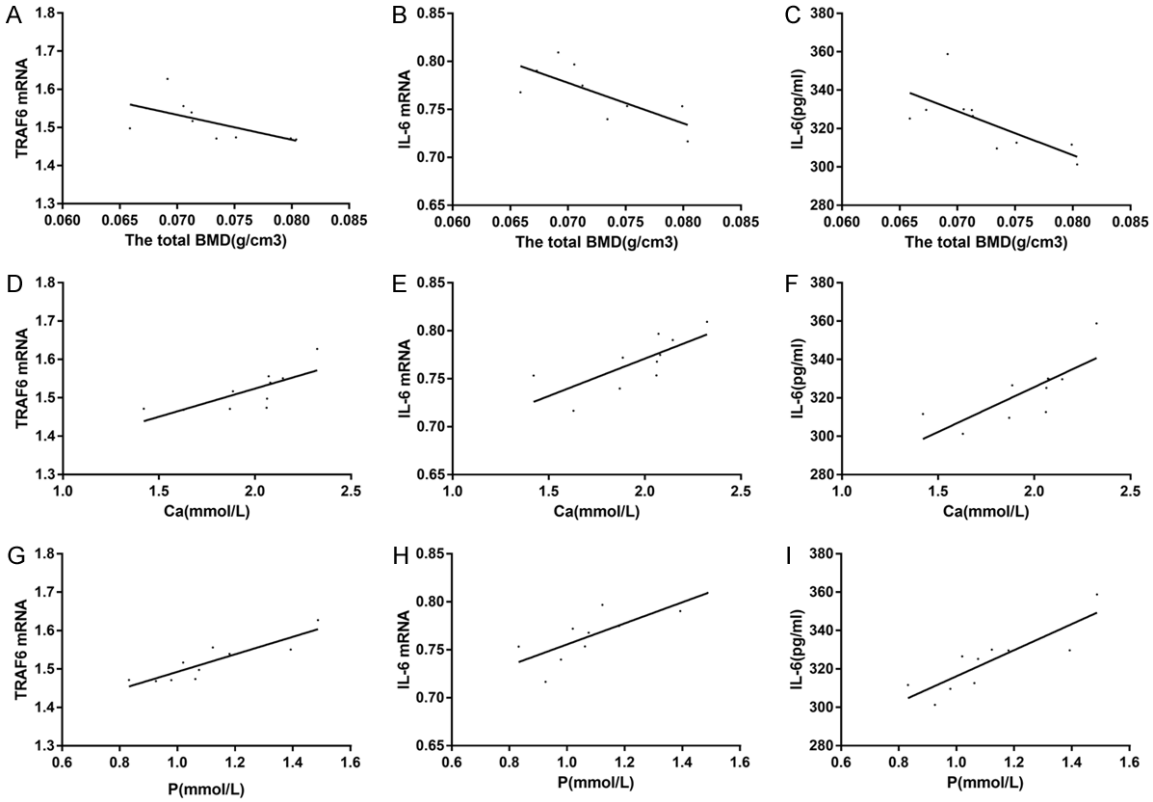

Figure 7. Analysis of correlations among measured factors. A: Correlation analysis of total bone density and *Traf6* mRNA, r=-0.615, P=0.039. B: Correlation analysis of total bone density and *Il6* mRNA, r=-0.740, P=0.015. C: Correlation analysis of total bone density and IL-6 protein abundance, r=-0.696, P=0.025. D: Correlation analysis of Ca^{2+} and *Traf6* mRNA, r=0.738, P=0.015. E: Correlation analysis of Ca^{2+} and *Il6* mRNA, r=0.811, P=0.004. F: Correlation analysis of Ca^{2+} and IL-6 protein abundance, r=0.732, P=0.016. G: Correlation analysis of P and *Traf6* mRNA, r=0.733, P=0.016. H: Correlation analysis of P and *Il6* mRNA, r=0.851, P=0.002. I: Correlation analysis of P and IL-6 protein abundance, r=0.765, P=0.010. Ca^{2+}, Calcium; P, Phosphorus; IL-6, interleukin-6; TRAF6, tumor necrosis factor receptor associated factor 6.

that the modeling was successful. Further, the difference in bone mineral density was more clear at 12 weeks after modeling. We also tracked bone mineral levels in the two groups of mice. In the sham-operation group, blood Ca^{2+} and P levels did not fluctuate significantly within 12 weeks after modeling, indicating that bone formation and bone resorption were in a dynamic equilibrium. By contrast, the levels of blood Ca^{2+} and P in mice of the model group gradually increased. At 3 weeks after modeling, the blood Ca^{2+} and P levels of model group mice did not show a significant change. This may be because the bones of the mice were still in the growth phase, so the bone mass had not yet reached peak level and the osteogenesis function was relatively strong, allowing a balance between bone formation and bone resorption with no clear effect of estrogen level fluctuations caused by ovariectomy [21].

The age of the mice used in this study was 65-75 days. In mice, 60-90 days from birth is the maturation period, and 120 days from birth

is the middle-age period [22]. Approximately 6 weeks after modeling, the mice began to enter the middle-age period and the levels of blood Ca^{2+} and P in the model group mice began to significantly increase. During this period, the mice in the model group could not compensate for the bone loss caused by ovariectomy, causing the blood Ca^{2+} and P levels to increase, and eventually resulted in osteoporosis. The basic mechanism of osteoporosis is an imbalance between bone resorption (osteoclast activity) and bone formation (osteoblast activity) [23]. At the same time, we detected the levels of *Traf6* mRNA, *Il6* mRNA, and IL-6 protein in the peripheral blood of mice, and found that in the model group, *Traf6* mRNA, *Il6* mRNA, and IL-6 protein were significantly higher compared to the sham-operation group.

TRAF6 is a member of the tumor necrosis factor receptor superfamily and is associated with the inhibition of the differentiation of bone marrow mesenchymal stem cells into osteoblasts. However, recent studies have stated that TRAF6 is closely related to the level of osteoclasts and that the downregulation of TRAF6 can inhibit osteoclastogenesis, thereby inhibiting bone loss [24]. IL-6 is a pleiotropic factor with multiple functions. Bone marrow mesenchymal stem cells can secrete IL-6, which increases the formation of osteoclasts via the interaction between osteoclasts and osteoblasts and increases bone resorption, leading to osteoporosis. Excessive secretion of IL-6 impairs the osteogenesis of osteoporotic bone marrow mesenchymal stem cells [25, 26]. Therefore, we used Spearman's correlation analysis to analyze the relationship between TRAF6, IL-6, bone mineral density, and bone minerals in model group mice at 12 weeks after surgery. *Traf6* mRNA, *IL6* mRNA, and IL-6 protein levels were all strongly and negatively correlated with bone mineral density; the higher the levels of *Traf6* and *Il6* mRNAs and IL-6 protein, the lower the bone density. In addition, *Traf6* and *Il6* mRNA and IL-6 protein levels showed strong positive correlations with blood Ca^{2+} and P levels, indicating that TRAF6 and IL-6 might disrupt the balance between bone formation and bone resorption in ovariectomized mice. This study also has certain limitations. Previous studies detected TRAF6 using western blot [27, 28]; however, owing to the limitations caused by the experimental conditions, here, we determined TRAF6 levels indirectly by detecting *Traf6* mRNA levels. Therefore, the changes in the levels of TRAF6 in osteoblasts and osteoclasts have not been analyzed in the present study, nor has the species difference between mice and humans been considered. Thus, results obtained in this study require further clinical verification.

In summary, TRAF6 and IL-6 may participate in the development of osteoporosis in ovariectomized osteoporotic mice by inhibiting bone formation, promoting bone resorption, and reducing bone density and thus disturbing the balance between bone formation and bone resorption.

Disclosure of conflict of interest

None.

Address correspondence to: Daiqin Chen, Department of Cardiology, Shaoyang Central Hospital, Shaoyang School of Meizilin Campus, College Road, Daxiang District, Shaoyang 422000, Hunan, China. Tel: +86-13907394138; E-mail: daiqqq8@163.com

References

[1] Moreira LD, Oliveira ML, Lirani-Galvao AP, Marin-Mio RV, Santos RN and Lazaretti-Castro M. Physical exercise and osteoporosis: effects of different types of exercises on bone and physical function of postmenopausal women. Arq Bras Endocrinol Metabol 2014; 58: 514-522.

[2] Khan A and Fortier M; Menopause and Osteoporosis Working Group. Osteoporosis in menopause. J Obstet Gynaecol Can 2014; 36: 839-840.

[3] Eriksen EF, Diez-Perez A and Boonen S. Update on long-term treatment with bisphosphonates for postmenopausal osteoporosis: a systematic review. Bone 2014; 58: 126-135.

[4] Tella SH and Gallagher JC. Prevention and treatment of postmenopausal osteoporosis. J Steroid Biochem Mol Biol 2014; 142: 155-170.

[5] Gambacciani M and Levancini M. Management of postmenopausal osteoporosis and the prevention of fractures. Panminerva Med 2014; 56: 115-131.

[6] McLendon AN and Woodis CB. A review of osteoporosis management in younger premenopausal women. Womens Health (Lond) 2014; 10: 59-77.

[7] Harris ST, Watts NB, Genant HK, McKeever CD, Hangartner T, Keller M, Chesnut CH 3rd, Brown J, Eriksen EF, Hoseyni MS, Axelrod DW and Miller PD. Effects of risedronate treatment on

vertebral and nonvertebral fractures in women with postmenopausal osteoporosis: a randomized controlled trial. Vertebral efficacy with risedronate therapy (VERT) study group. JAMA 1999; 282: 1344-1352.
[8] Baccaro LF, Conde DM, Costa-Paiva L and Pinto-Neto AM. The epidemiology and management of postmenopausal osteoporosis: a viewpoint from Brazil. Clin Interv Aging 2015; 10: 583-591.
[9] Zhang Y, Liu M, Li H, Chen Z, Liang N, Xu J, Zhang X and Zhang Y. Traditional Chinese medicine Bushen-Jianpi-Huoxue decoction prevents diabetic osteoporosis in rats via Wnt and nuclear factor-kappa B signaling pathways. Int J Rheum Dis 2017; 20: 941-948.
[10] Yan L, Hu R, Tu S, Cheng WJ, Zheng Q, Wang JW, Kan WS and Ren YJ. Meta-analysis of association between IL-6-634C/G polymorphism and osteoporosis. Genet Mol Res 2015; 14: 19225-19232.
[11] He H, Xu F, Huang W, Luo S, Lin Y, Zhang G, Du Q and Duan R. miR-125a-5p expression is associated with the age of breast cancer patients. Genet Mol Res 2015; 14: 17927-17933.
[12] Cosman F, de Beur SJ, LeBoff MS, Lewiecki EM, Tanner B, Randall S and Lindsay R; National Osteoporosis Foundation. Clinician's guide to prevention and treatment of osteoporosis. Osteoporos Int 2014; 25: 2359-2381.
[13] Black DM and Rosen CJ. Postmenopausal osteoporosis. N Engl J Med 2016; 374: 2096-2097.
[14] Straka M, Straka-Trapezanlidis M, Deglovic J and Varga I. Periodontitis and osteoporosis. Neuro Endocrinol Lett 2015; 36: 401-406.
[15] Clarke BL. Anti-sclerostin antibodies: utility in treatment of osteoporosis. Maturitas 2014; 78: 199-204.
[16] Nakamura I, Duong LT, Rodan SB and Rodan GA. Involvement of alpha(v)beta3 integrins in osteoclast function. J Bone Miner Metab 2007; 25: 337-344.
[17] Lin CC, Li TC, Liu CS, Yang CW, Lin CH, Hsiao JH, Meng NH, Lin WY, Liao LN, Li CI and Wu FY. Associations of TNF-alpha and IL-6 polymorphisms with osteoporosis through joint effects and interactions with LEPR gene in Taiwan: Taichung Community Health Study for Elders (TCHS-E). Mol Biol Rep 2016; 43: 1179-1191.
[18] Cao H, Zhang Y, Qian W, Guo XP, Sun C, Zhang L and Cheng XH. Effect of icariin on fracture healing in an ovariectomized rat model of osteoporosis. Exp Ther Med 2017; 13: 2399-2404.
[19] Han H, Peng J, Hong Y, Fu Z, Lu K, Li H, Zhu C, Zhao Q and Lin J. Comparative characterization of microRNAs in Schistosoma japonicum schistosomula from Wistar rats and BALB/c mice. Parasitol Res 2015; 114: 2639-2647.
[20] Qaseem A, Forciea MA, McLean RM and Denberg TD; Clinical Guidelines Committee of the American College of Physicians. Treatment of low bone density or osteoporosis to prevent fractures in men and women: a clinical practice guideline update from the American college of physicians. Ann Intern Med 2017; 166: 818-839.
[21] Tsai TT, Tai CL, Ho NY, Lai PL, Fu TS, Niu CC, Chen LH and Chen WJ. Effects of strontium ranelate on spinal interbody fusion surgery in an osteoporotic rat model. PLoS One 2017; 12: e0167296.
[22] Ghasemi S, Hosseini M, Feizpour A, Alipour F, Sadeghi A, Vafaee F, Mohammadpour T, Soukhtanloo M, Ebrahimzadeh Bideskan A and Beheshti F. Beneficial effects of garlic on learning and memory deficits and brain tissue damages induced by lead exposure during juvenile rat growth is comparable to the effect of ascorbic acid. Drug Chem Toxicol 2017; 40: 206-214.
[23] McClung MR, Grauer A, Boonen S, Bolognese MA, Brown JP, Diez-Perez A, Langdahl BL, Reginster JY, Zanchetta JR, Wasserman SM, Katz L, Maddox J, Yang YC, Libanati C and Bone HG. Romosozumab in postmenopausal women with low bone mineral density. N Engl J Med 2014; 370: 412-420.
[24] Tan EM, Li L, Indran IR, Chew N and Yong EL. TRAF6 mediates suppression of osteoclastogenesis and prevention of ovariectomy-induced bone loss by a novel prenylflavonoid. J Bone Miner Res 2017; 32: 846-860.
[25] Li X, Zhou ZY, Zhang YY and Yang HL. IL-6 contributes to the defective osteogenesis of bone marrow stromal cells from the vertebral body of the glucocorticoid-induced osteoporotic mouse. PLoS One 2016; 11: e0154677.
[26] Kim MH, Jung K, Nam KH, Jang HJ, Lee SW, Kim Y, Park CS, Lee TH, Park JH, Choi JH, Rho MC and Oh HM. Salvia plebeia R.Br. inhibits signal transduction of IL-6 and prevents ovariectomy-induced bone loss by suppressing osteoclastogenesis. Arch Pharm Res 2016; 39: 1671-1681.
[27] Sun H, Gong Y, Qiu J, Chen Y, Ding F and Zhao Q. TRAF6 inhibition rescues dexamethasone-induced muscle atrophy. Int J Mol Sci 2014; 15: 11126-11141.
[28] Walsh MC, Lee J and Choi Y. Tumor necrosis factor receptor-associated factor 6 (TRAF6) regulation of development, function, and homeostasis of the immune system. Immunol Rev 2015; 266: 72-92.